

Steady-State Free-Precession Sequence for Differentiating Bronchogenic Carcinoma from Adjacent Atelectasis

Tsukasa Saida*, Seiji Shiotani, Kensaku Mori, Tomoya Kobayashi, Hiroichi Ishikawa, Hideo Ichimura and Manabu Minami

Department of Radiology, Faculty of Medicine, University of Tsukuba, Japan

*Corresponding author: Tsukasa Saida, Department of Radiology, Faculty of Medicine, University of Tsukuba, 1-1-1 Tennodai, Tsukuba Ibaraki, 305-8575, Japan, Tel: 81-29-853-3205; E-mail: saida_sasaki_tsukasa@yahoo.co.jp

Received date: December 03, 2015; Accepted date: January 08, 2016; Published date: January 11, 2016

Copyright: © 2016 Saida T, et al. This is an open-access article distributed under the terms of the Creative Commons Attribution License, which permits unrestricted use, distribution, and reproduction in any medium, provided the original author and source are credited.

Abstract

Purpose: To evaluate the clinical usefulness of steady-state free-precession (SSFP) sequence for differentiating bronchogenic carcinoma from adjacent atelectasis.

Methods: Ten patients with bronchogenic carcinoma and adjacent atelectasis underwent unenhanced magnetic resonance imaging (MRI). MRI examinations using the SSFP sequence, T2-weighted imaging (T2WI), and diffusion-weighted imaging (DWI) ($b=0, 1000 \text{ s/mm}^2$) were performed on a 1.5-T scanner. Two independent observers evaluated the differentiating ability and image quality using 3-point scales. In addition, the relative contrast of carcinoma and atelectasis in the SSFP sequence and T2WI and apparent diffusion coefficient (ADC) of DWI were calculated. Statistical analyses were performed using the t-test, Friedman test, Wilcoxon test and analysis of variance.

Results: The SSFP sequence showed significantly higher differentiating ability than T2WI ($P=0.004$) and significantly better image quality than T2WI ($P<0.001$) and DWI ($P=0.005$). There was a significant difference between the relative contrasts and the ADC values of carcinoma and atelectasis on all sequences (SSFP sequence, $P=0.034$; T2WI, $P=0.010$ and ADC, $P<0.001$).

Conclusion: The SSFP sequence has the advantages of short acquisition times, which avoid motion artifacts, and relatively good contrast, which provides detailed anatomical information. It can be considered as a useful modality for differentiating bronchogenic carcinoma from adjacent atelectasis.

Keywords: SSFP; Lung tumor; Collapsed lung; Diffusion-weighted image; Unenhanced; Non-contrast; Magnetic resonance imaging

Introduction

Advanced central bronchogenic carcinoma often accompanies adjacent obstructive atelectasis [1]. Differentiation between bronchogenic carcinoma and adjacent atelectasis is necessary to determine the true tumor size and field of radiation therapy or to evaluate the effects of radiation and chemotherapy. At present, contrast-enhanced computed tomography (CT) is the gold-standard modality for evaluating bronchogenic carcinoma; however, it is often difficult to distinguish bronchogenic carcinoma from atelectasis [1,2]. Recently, magnetic resonance imaging (MRI) using diffusion-weighted imaging (DWI) has been reported to be a useful modality for this purpose [1,3,4], but its motion artifacts due to the heartbeat and susceptibility artifacts due to the aerated lung deteriorates the image quality of DWI, and the anatomical information on DWI is insufficient. Steady-state free-precession (SSFP) sequence is based on a low-flip angle gradient-echo sequence with a high spatial resolution and short acquisition time. Therefore, we attempted to apply the SSFP sequence for this purpose. The aim of this study was to evaluate the clinical usefulness of the SSFP sequence for differentiating bronchogenic carcinoma from adjacent atelectasis.

Materials and Method

Patients

This retrospective study was approved by the institutional review board and the informed consent requirement was waived. From July 2011 to November 2012, 10 patients with bronchogenic carcinoma and adjacent atelectasis who were referred to our hospital satisfied the inclusion criteria of the study. The inclusion criteria were as follows: 1) diagnosis of bronchogenic carcinoma with adjacent atelectasis on unenhanced or contrast-enhanced CT and 2) histopathological proof of bronchogenic carcinoma. The exclusion criteria were as follows: 1) any contraindication for participation in a magnetic resonance imaging (MRI) study including claustrophobia and implanted metallic devices, such as cardiac pacemakers; 2) previous treatment experience, such as chemotherapy and radiotherapy and 3) critical patient situations that prevent participation in a breath-hold MRI study.

The study group included 10 patients comprising 9 men and 1 woman whose ages ranged from 58 to 82 years (mean, 70 years). Bronchogenic carcinomas were histopathologically proven by bronchoscopy biopsy in 9 patients and by autopsy in 1 patient. Contrast-enhanced CT was performed in 6 patients, and only unenhanced CT was performed in the other 4 patients because of renal failure.

Imaging protocol

An unenhanced MRI study was performed on a 1.5-T MRI system (Magnetom Avanto; Siemens, Erlangen, Germany) using a 6-element phased-array body coil and a spine coil. The MRI protocol included 3 imaging sequences. First, an axial two-dimensional (2D) SSFP sequence was acquired with the following imaging parameters: repetition time (TR)/echo time (TE), 3.69 ms/1.53 ms; flip angle, 63°; field of view (FOV), 200–267 × 267 mm; matrix, 192–256 × 256; number of slices, 20–37; slice thickness, 5 mm; slice gap, 0.5 mm and total scan duration, 14–25 s. This sequence was acquired while the patient performed a breath hold. Second, an axial T2-weighted imaging (T2WI) sequence using a fast-spine echo method was obtained with the following imaging parameters: TR/TE, 2020–3390 ms/113–114 ms; flip angle, 150°; FOV, 287 × 250 mm; matrix, 320 × 168–259; number of slices, 20–37; slice thickness, 5 mm; slice gap, 0.5 mm and acquisition time, (20–37sec) × 2. This sequence was acquired during 2 breath holds. Third, a DWI sequence with b=0, 1000 s/mm² was acquired with the following imaging parameters: TR/TE, 3500–7236 ms/77–83 ms; flip angle, 90°; FOV, 215 × 300 mm; matrix, 74–83 × 128; number of slices, 20–37; slice thickness, 5 mm; slice gap, 1 mm and total scan duration, 3 min 25 s to 5 min 19 s. This sequence was acquired using a respiration-triggered technique. In cases with respiratory distress, an MRI study was performed under oxygen administration.

CT was performed using a 16-slice multidetector scanner (Aquilion 16; Toshiba Medical Systems, Tokyo, Japan). Images were obtained under the following conditions: 120 kV; 450 mAs/slice; pitch, 0.390; variable FOV; matrix, 512 × 512; collimation, 0.390 × 16 mm and reconstruction thickness, 1 mm. The maximum interval between CT and the subsequent MRI study was 42 days (mean, 12.5 days).

Image analysis

For qualitative analysis, 2 independent observers (A, a radiologist with 20 years of experience, and B, a radiologist with 10 years of experience) evaluated the differentiating ability and the image quality, including absence of artifacts and deformation, using a 3-point scale (poor, 0; moderate, 0.5; good, 1.0). For evaluating the differentiating ability, cases in which the tumor and atelectasis could not be differentiated were considered to be poor, cases in which the tumor and atelectasis could be differentiated but had some poorly defined boundaries were considered to be moderate and cases in which clear boundaries were observed between the tumor and atelectasis were considered to be good. For evaluating the image quality, images that were non diagnostic because of artifacts were considered to be poor, images that were diagnostic despite some artifacts were considered to be moderate and images with no artifacts were considered to be good. All MRI were analysed on a PVR workstation (PVR version 1.94; Toshiba Medical Systems, Tokyo, Japan). For quantitative analysis, region of interest (ROI) analyses were performed. The ROIs were placed on the areas that were definitely considered to be carcinoma and atelectasis (Figure 1).



Figure 1: ROIs are placed on the areas definitely considered to be bronchogenic carcinoma and atelectasis.

If there was no necrotic area in the tumor, the ROIs were placed on the center of the bronchogenic carcinoma, and if the tumor contained necrosis, the ROIs were placed on the viable area of the carcinoma by avoiding the cystic area. The cystic area in the tumor was defined as unenhanced lesion on contrast-enhanced CT or the high signal intensity on T2WI. The relative contrast (RC) to the background on the SSFP sequence and T2WI and the mean ADC values of DWI were calculated for bronchogenic carcinoma and adjacent atelectasis. RC was calculated according to the following equation:

$$RC = \text{Signal intensity (SI) of the tumor or atelectasis} / \text{SI of the background lung}$$

The ADC maps were automatically reconstructed for all DWI images, and the mean ADC values were measured on ADC maps for each ROI. Differentiation of bronchogenic carcinoma from adjacent atelectasis was achieved by the analysis of a combination of CT and all the MRI sequences after reaching a consensus between the 2 observers.

Statistical analysis

Statistical analyses were performed using dedicated software (SPSS, version 19.0 for Windows). For qualitative analysis, the Friedman test, Wilcoxon test and analysis of variance (ANOVA) were performed. For quantitative analysis, the statistical significance test in RCs and ADC values between bronchogenic carcinoma and atelectasis was performed using the t-test. A P value of <0.05 was considered to indicate a statistically significant difference.

Results

MRI studies were technically successful in all 10 patients. Because the total in-room time was less than 20 min, the procedure was well tolerated by all patients. The histopathological types of bronchogenic carcinoma were squamous carcinoma in 6 patients, adenocarcinoma in 3 patients and small-cell carcinoma in 1 patient. Tumor sizes ranged from 40 to 97 mm (mean, 65.7 mm) in the axial plane from the SSFP sequence data. Atelectatic areas were less than one-third of the lobe in 6 patients and more than one-third and less than two-thirds of the lobe in 4 patients. Tumors were located in the left upper lobe in 3 patients, in the left lower lobe in 4, in the right upper lobe in 2 and in the right lower lobe in 1.

Bronchogenic carcinoma showed hypointensities relative to the intensities of atelectasis on the SSFP sequence, T2WI and the ADC map. On DWI ($b=1000 \text{ s/mm}^2$) bronchogenic carcinoma showed hyperintensities relative to the intensities of atelectasis (Figures 2 and 3).

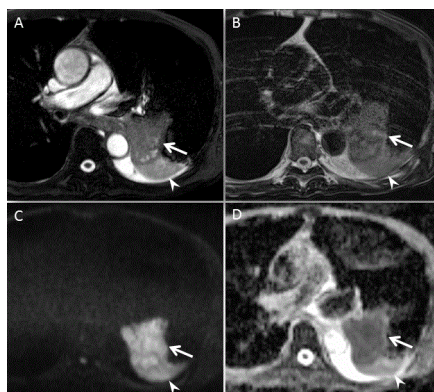


Figure 2: A 78-year-old man with squamous cell carcinoma in the left lower lobe. SSFP sequence (A), T2WI (B), DWI with b value of 1000 s/mm^2 (C) and ADC map (D). Bronchogenic carcinoma (arrows) and adjacent atelectasis (arrowheads) are clearly differentiated on both the SSFP sequence and ADC map. T2WI shows motion artifact due to the heartbeat.

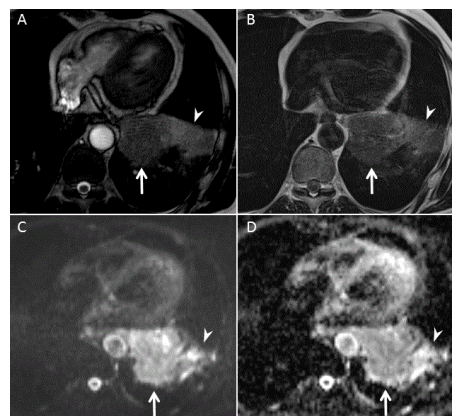


Figure 3: A 58-year-old man with squamous cell carcinoma in the left lower lobe. SSFP sequence (A), T2WI (B), DWI with b value of 1000 s/mm^2 (C) and ADC map (D). Bronchogenic carcinoma (arrows) and adjacent atelectasis (arrowheads) are clearly differentiated on the SSFP sequence. T2WI shows motion artifact due to the heartbeat and poor contrast between bronchogenic carcinoma and atelectasis. DWI and the ADC map show image distortion.

The comparison of the differentiating ability and image quality of the SSFP sequence, T2WI and DWI ($b=1000 \text{ s/mm}^2$) +ADC map are shown in Tables 1 and 2. The differentiating ability was significantly higher for the SSFP sequence than for T2WI. The image quality was significantly higher for the SSFP sequence than for T2WI and the DWI ($b=1000 \text{ s/mm}^2$) +ADC map. In the ANOVA results, the observer difference did not have an influence.

Case	Differentiating ability (Observer A/B)			Image quality (Observer A/B)		
	SSFP	T2WI	DWI+ADC	SSFP	T2WI	DWI+ADC
1	1.0/1.0	1.0/1.0	1.0/1.0	1.0/1.0	0.5/0.5	1.0/0.5
2	1.0/1.0	0/0	1.0/1.0	1.0/1.0	0.5/0.5	1.0/1.0
3	1.0/0.5	1.0/1.0	1.0/1.0	1.0/1.0	0.5/0.5	1.0/1.0
4	1.0/1.0	0/0	1.0/1.0	1.0/1.0	0.5/0	1.0/0.5
5	1.0/1.0	1.0/1.0	1.0/1.0	1.0/1.0	1.0/1.0	1.0/1.0
6	0.5/0.5	0/0	1.0/1.0	1.0/1.0	0/0	1.0/0.5
7	1.0/1.0	0/0	0.5/0.5	1.0/1.0	0.5/0	0.5/0.5
8	1.0/1.0	1.0/1.0	1.0/1.0	1.0/1.0	0.5/0.5	0.5/0.5
9	1.0/1.0	1.0/0.5	1.0/1.0	1.0/1.0	0.5/0.5	0.5/1.0
10	1.0/1.0	0/0.5	1.0/1.0	1.0/1.0	0/0.5	1.0/1.0
Mean score	0.95/0.90	0.5/0.5	0.95/0.95	1.0/1.0	0.45/0.40	0.85/0.75

Table 1: The differentiating ability and image quality of the SSFP sequence, T2WI and DWI ($b=1000 \text{ s/mm}^2$) +ADC map for each case (poor 0, moderate 0.5, good 1.0).

Sequence	Differentiating ability		Image quality	
SSFP	0.925	P=0.004	1.00	P<0.001
T2WI	0.50		0.43	
DWI+ADC	0.95	P=0.002	0.80	P=0.001

Table 2: Comparison of the differentiating ability and image quality of the SSFP sequence, T2WI and DWI (b=1000 s/mm²) +ADC map (poor 0, moderate 0.5, and good 1.0).

In quantitative analysis, there was a significant difference between RCs of bronchogenic carcinoma and those of atelectasis on the SSFP sequence (P=0.034) and T2WI (P=0.010) (Table 3). There was also a

significant difference between the mean ADC values of bronchogenic carcinoma and those of atelectasis (P<0.001).

	SSFP(RC)			T2WI(RC)			ADC		
	Mean	SD	P	Mean	SD	P	Mean	SD	P
Tumor	15.75	5.99	0.034	5.43	1.76	0.010	101.07	30.41	<0.001
Atelectasis	27.38	18.02		10.47	5.94		960.87	247.06	

SD=standard deviation

Table 3: RCs and the mean ADC values of bronchogenic carcinoma and atelectasis.

The ratios of bronchogenic carcinoma to atelectasis on the signal intensities of the SSFP sequence and T2WI and on the mean ADC values are shown in Figure 4. The median and standard deviation of each ratio were 0.69 and 0.19 on the SSFP sequence, 0.64 and 0.19 on T2WI and 0.10 and 0.09 on the mean ADC, respectively.

adjacent atelectasis is clinically important for therapy, including radiation therapy and chemotherapy. Contrast-enhanced CT is the gold standard examination for evaluating bronchogenic carcinoma, and dynamic contrast-enhanced CT has been shown to distinguish bronchogenic carcinoma from atelectasis in approximately 80% of the study cases examined [5]. Nevertheless, on bolus contrast-enhanced CT, enhancement of atelectasis often appears similar to that of bronchogenic carcinoma, which prevents differentiation [1,2]. Therefore, the differentiating ability of bolus contrast-enhanced CT, the gold standard modality for evaluating the extent of bronchogenic carcinoma, is poor.

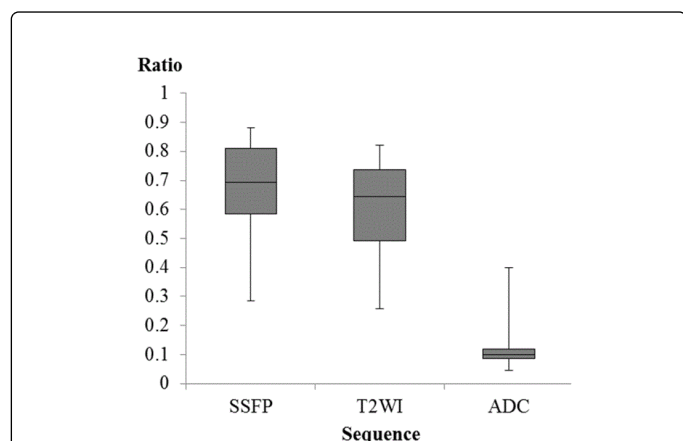


Figure 4: The ratios of bronchogenic carcinoma to atelectasis (the signal intensities of SSFP, T2WI and the mean ADC values; tumor/atelectasis). The ratio of bronchogenic carcinoma to adjacent atelectasis is relatively lower on the mean ADC than on the signal intensity of SSFP sequence and T2WI. The ratio of the signal intensity on the SSFP is similar to that on T2WI.

Discussion

Advanced bronchogenic carcinoma often accompanies adjacent atelectasis, and differentiation between bronchogenic carcinoma and

MRI has the potential to differentiate bronchogenic carcinoma from atelectasis without contrast media, and several MRI studies have evaluated the potential of conventional image sequences, including T1WI and T2WI [5-8]. However, some researchers have reported that the *in vivo* values of T1 and T2 for malignant tumors overlap with those of benign processes of lung parenchyma [8-10]. Recently, DWI has been reported to be a useful modality for detecting bronchogenic carcinoma [11-14] and for differentiating bronchogenic carcinoma from atelectasis [1,3,4]. Nevertheless, motion artifacts due to the heartbeat and breathing and susceptibility artifacts due to the air in the lung deteriorate the image quality of DWI; moreover, the spatial resolution of DWI is low, and the anatomical information of DWI is insufficient.

Therefore, in the present study, we investigated the potential of the 2D SSFP sequence using the breath-hold technique for the ability to differentiate between bronchogenic carcinoma and atelectasis. There are a few reports on the feasibility of imaging using the SSFP sequence in the lung [15-18], and Rajaram et al. showed that there was a potential role for the SSFP sequence as a noncontract imaging modality in the lung. The image contrast of the SSFP sequence depends on the T2/T1 ratio, and the advantages of the SSFP sequence are its short acquisition time, which avoids motion artifacts, and its

inherently high contrast. In addition, the SSFP sequence provides detailed anatomical information. Moreover, because the 2D SSFP sequence is the most fundamental sequence and requires no special technique, we believe that it is feasible to use on any MRI instrument. In our study, the SSFP sequence and DWI showed significantly better abilities for distinguishing bronchogenic carcinoma from atelectasis than T2WI. In addition, comparison of the image quality showed that the SSFP sequence gave significantly better results than DWI and T2WI. Post-obstructive atelectasis is composed of collapsed lung, bronchial impaction and pneumonia. The differentiating ability of T2WI was relatively poor because organizing pneumonitis and atelectasis are usually isointense with the tumor, which prevents differentiation on T2WI. In contrast, cholesterol pneumonitis and bronchiectasis with mucus plugs are usually hyper intense relative to the intensity of tumors, which enables differentiation on T2WI sequence [6,19].

ADC values have been shown to be correlated with tumor cellularity. Matoba et al [11] reported that the ADC values of bronchogenic carcinomas correlated well with tumor cellularity. In this study, we selected a b value of 1000 s/mm², a value used in previous studies [3,12-14]. In contrast to previous studies [1,3,4] that evaluated the feasibility of DWI for differentiating bronchogenic carcinoma from atelectasis, we applied a respiration-triggered technique to avoid misregistration artifacts due to breath-hold instability in multiple breath holds. These verification conditions resulted in better image quality for differentiating bronchogenic carcinoma from atelectasis.

Our study had several limitations. First, the study population was relatively small. Further investigation in a larger patient population is needed to confirm our results. Second, no radiological-pathological correlation analysis was performed because all patients had advanced inoperable bronchogenic carcinoma. Third, the study was retrospective and contained several biases.

In conclusion, although CT is the first-choice imaging modality even in cases of bronchogenic carcinoma associated with adjacent atelectasis, our preliminary study results showed that the abilities of the SSFP sequence to differentiate between bronchogenic carcinoma and adjacent atelectasis were equal to that of DWI and better than that of T2WI. The SSFP sequence did not require the use of a contrast medium or the higher radiation exposure inherent with CT. In addition, the SSFP sequence provided the best detailed anatomical information because of its higher spatial resolution and better image quality.

References

1. Qi LP, Zhang XP, Tand L, Li J, Sun YS, et al. (2009) Using diffusion-weighted MR imaging for tumor detection in the collapsed lung: a preliminary study. *Eur Radiol* 19: 333-341.
2. Verschakelen JA, Bogaert J, De Weaver W (2002) Computed tomography in staging for lung cancer. *Eur Respir J* 19: 40-48.
3. Baysal T, Mutlu DY, Yologlu S (2009) Diffusion-weighted magnetic resonance imaging in differentiation of postobstructive consolidation from central lung carcinoma. *Magn Reson Imaging* 27: 1447-1454.
4. Yang RM, Li L, Wei XH, Guo YM, Huang YH, et al. (2013) Differentiation of central lung cancer from atelectasis: comparison of diffusion-weighted MRI with PET/CT. *PLoS One* 8: e60279.
5. Tobler J, Levitt RG, Glazer HS, Moran J, Crouch E, et al. (1987) Differentiation of proximal bronchogenic carcinoma from postobstructive lobar collapse by magnetic resonance imaging. Comparison with computed tomography. *Invest Radiol* 22: 538-543.
6. Bourgouin PM, Mcloud TC, Fitzgibbon JF, Mark EJ, Shepard JA, et al. (1991) Differentiation of bronchogenic carcinoma from postobstructive pneumonitis by magnetic resonance imaging: histopathologic correlation. *J Thorac Imaging* 6: 22-27.
7. Onitsuka H, Tsukuda M, Araki A, Murakami J, Torii Y, et al. (1991) Differentiation of central lung tumor from postobstructive lobar collapse by rapid sequence computed tomography. *J Thorac Imaging* 6: 28-31.
8. Shioya S, Haida M, Ono Y, Fukuzaki M, Yamabayashi H (1988) Lung cancer: differentiation of tumor, necrosis, and atelectasis by means of T1 and T2 values measured *in vitro*. *Radiology* 167: 105-109.
9. Ross JS, O'Donovan PB, Novoa R, et al. (1984) Magnetic resonance of the chest: initial experience with imaging and *in vivo* T1 and T2 calculations. *Radiology* 52: 95-101.
10. Moore EH, Webb WR, Muller N, Sollitto R (1986) MRI of pulmonary airspace disease: experimental model and preliminary clinical results. *AJR Am J Roentgenol*; 146: 1123-1128.
11. Matoba M, Tonami H, Kondou T, Yokota H, Higashi K, et al. (2007) Lung carcinoma: diffusion weighted MR imaging—preliminary evaluation with apparent diffusion coefficient *Radiology* 243: 570-577.
12. Ohno Y, Koyama H, Onishi Y, Takenaka D, Nogami M, et al. (2008) Nonsmall cell lung cancer: whole-body MR examination for M-stage assessment— utility for whole-body diffusion-weighted imaging compared with integrated FDG PET/CT. *Radiology* 248: 643-654.
13. Razeq AA (2012) Diffusion magnetic resonance imaging of chest tumors. *Cancer Imaging* 12: 452-463.
14. Gümüştaş S, Inan N, Akansel G, Ciftçi E, Demirci A, et al. (2012) Differentiation of malignant and benign lung lesions with diffusion-weighted MR imaging. *Radiol Oncol* 46: 106-113.
15. Rajaram S, Swift AJ, Capener D, Telfer A, Davies C, et al. (2012) Lung morphology assessment with balanced steady-state free precession MR imaging compared with CT. *Radiology* 263: 569-577.
16. Sawant A, Keall P, Pauly KB, Alley M, Vasanaawala S, et al. (2014) Investigating the feasibility of rapid MRI for image-guided motion management in lung cancer radiotherapy. *Biomed Res Int* 2014: 485067.
17. Fabel M, Wintersperger BJ, Dietrich O, Eichinger M, Fink C, et al. (2009) MRI of respiratory dynamics with 2D steady-state free-precession and 2D gradient echo sequences at 1.5 and 3 Tesla: an observer preference study. *Eur Radiol* 19: 391-399.
18. Failo R, Wielopolski PA, Tiddens HA, Hop WC, Mucelli RP, et al. (2009) Lung morphology assessment using MRI: a robust ultra-short TR/TE 2D steady state free precession sequence used in cystic fibrosis patients. *Magn Reson Med* 61: 299-306.
19. Glazer HS, Anderson DJ, Sagel SS (1989) Bronchial impaction in lobar collapse: CT demonstration and pathologic correlation. *AJR Am J Roentgenol* 153: 485-488.